Mechanical Systems and Signal Processing (1999) **13**(6), 855–878
Article No. mssp.1999.1249, available online at http://www.idealibrary.com on IDEAL®

REFERENCE-BASED STOCHASTIC SUBSPACE IDENTIFICATION FOR OUTPUT-ONLY MODAL ANALYSIS

BART PEETERS AND GUIDO DE ROECK

Department of Civil Engineering, Katholieke Universiteit Leuven, Leuven, Belgium.
E-mail: bart.peeters@bwk.kuleuven.ac.be

(Received 17 December 1998, revised 2 June 1999, accepted 23 July 1999)

When performing vibration tests on civil engineering structures, it is often unpractical and expensive to use artificial excitation (shakers, drop weights). Ambient excitation on the contrary is freely available (traffic, wind), but it causes other challenges. The ambient input remains unknown and the system identification algorithms have to deal with output-only measurements. For instance, realisation algorithms can be used: originally formulated for impulse responses they were easily extended to output covariances. More recently, data-driven stochastic subspace algorithms which avoid the computation of the output covariances were developed. The key element of these algorithms is the projection of the row space of the future outputs into the row space of the past outputs. Also typical for ambient testing of large structures is that not all degrees of freedom can be measured at once but that they are divided into several set-ups with overlapping reference sensors. These reference sensors are needed to obtain global mode shapes. In this paper, a novel approach of stochastic subspace identification is presented that incorporates the idea of the reference sensors already in the identification step: the row space of future outputs is projected into the row space of past reference outputs. The algorithm is validated with real vibration data from a steel mast excited by wind load. The price paid for the important gain concerning computational efficiency in the new approach is that the prediction errors for the non-reference channels are higher. The estimates of the eigenfrequencies and damping ratios do not suffer from this fact.

I. INTRODUCTION

In-operation system identification is a very relevant topic in civil engineering. For bridge monitoring based on damage identification methods that need the dynamic characteristics of the structure, the only efficient way to obtain these characteristics is in-operation modal analysis. The bridge was available for public use during the measurements and it was impossible to change the boundary conditions to obtain an ideal free-free set-up. So the use of artificial shaker or impact excitation is not very practical: in most cases at least one lane has to be closed and secondary excitation sources, having a negative effect on the data quality, cannot be excluded: traffic under/on the bridge, wind, micro tremors [1]. For output-only system identification, on the other hand, these ambient excitation sources are essential. By using such stochastic and unmeasurable ambient excitation, the traditional frequency response function or impulse response function based modal parameter estimation methods are excluded, since they rely on both input and output measurements.

A widely used method in civil engineering to determine the eigenfrequencies of a structure based on output-only measurements is the rather simple peak-picking method. In this method, the measured time histories are converted to spectra by a discrete Fourier transform (DFT). The eigenfrequencies are simply determined as the peaks of the spectra.

0888–3270/99/110855 + 24 $30.00/0

Mode shapes can be determined by computing the transfer functions between all outputs and a reference sensor. A practical implementation of this method was realised by Felber [2]. The major advantage of the method is its speed: the identification can be done on-line allowing a quality check of the acquired data on site. Disadvantages are the subjective selection of eigenfrequencies, the lack of accurate damping estimates and the determination of operational deflection shapes instead of mode shapes, since no modal model is fitted to the data.

Therefore, we are looking for more advanced methods. Literature exists on several system identification methods that can identify systems excited by unknown input. The detailed knowledge of the excitation is replaced by the assumption that the system is excited by white Gaussian noise. The most general model of a linear time-invariant system excited by white noise is the so-called ARMAV-model: the autoregressive term of the outputs is related to a moving average term of the white noise inputs. Based on the measurements, the prediction error method [3] is able to solve for the unknown matrix parameters. Unfortunately, this method results in a highly non-linear minimisation problem with related problems such as: convergence not being guaranteed, local minima, sensitivity to initial values and especially in the case of multivariable systems, an almost unreasonable computational burden [4, 5]. One possible solution is to omit the moving average terms of an ARMAV-model that cause the non-linearity and to solve a linear least-squares problem to find the parameters of an ARV-model. A disadvantage is that since this model is less general, an overspecification of the model order is needed which results in a number of spurious numerical modes. The stochastic subspace system identification method [6] shares the advantages of both the above-mentioned methods: the identified model is a stochastic state-space model which is in fact a transformed ARMAV-model, and as such more general than the ARV-model; the identification method does not involve any non-linear calculations and is therefore much faster and more robust than the prediction error method.

There has been much work on output-only identification. Benveniste and Fuchs [7] considered as early as in 1985 the use of stochastic realisation algorithms (Section 4) for modal analysis of structures (Section 7.1). Another interesting result of Benveniste and Fuchs [7] is the extension to the non-stationary white noise case. More results and applications are given in [8, 9]. Another application of subspace identification, in addition to the determination of modal parameters, is the use of the so-called level 1 damage detection (for answering the question whether there is structural damage or not). This subject is treated in [10, 11]. Several applications of output-only identification have been reported: modal analysis of aircraft structures [12]; health monitoring of a sports car [13]; and identification of offshore platforms [14]. As an alternative for output-only time domain methods, Guillaume *et al.* [15] have developed the maximum likelihood identification that operates in the frequency domain. In contrast to the peak-picking method that does not really imply any parametric modelling, a modal model is fitted to the output spectra. Peeters *et al.* [16] are reporting on the comparison of several output-only identification methods when applied to bridge vibration data.

The paper is organised as follows. Section 2 discusses the state-space modelling of vibrating structure. Section 3 gives some well-known properties of stochastic state-space models; also some notations are clarified, needed in the discussion of the stochastic realisation algorithm (Section 4) and the stochastic subspace algorithm (Section 5). Both algorithms are variants of the classical implementations in the sense that in the stochastic realisation algorithm of section 4 only the covariances between the outputs and a set of references are needed. The algorithm of Section 5 is a data-driven subspace translation of this algorithm. In Section 6, the approaches of the two previous sections are compared. Section 7 explains how the identification results can be used in modal and spectrum

analysis. Finally, Section 8 discusses a practical application of the theory: a steel mast excited by wind load is analysed.

2. STATE-SPACE MODELLING OF VIBRATING STRUCTURES

The dynamic behaviour of a discrete mechanical system consisting of n_2 masses connected through springs and dampers is described by the following matrix differential equation:

$$M\ddot{U}(t) + C_2\dot{U}(t) + KU(t) = F(t) = B_2u(t) \tag{1}$$

where M, C_2, $K \in \mathbb{R}^{n_2 \times n_2}$ are the mass, damping and stiffness matrices, $F(t) \in \mathbb{R}^{n_2 \times 1}$ is the excitation force, and $U(t) \in \mathbb{R}^{n_2 \times 1}$ is the displacement vector at continuous time t. Observe that the force vector $F(t)$ is factorised into a matrix $B_2 \in \mathbb{R}^{n_2 \times m}$ describing the inputs in space and a vector $u(t) \in \mathbb{R}^{m \times 1}$ describing the m inputs in time. For systems with distributed parameters (e.g. civil engineering structures), this equation is obtained as the finite element approximation of the system with only n_2 degrees of freedom (dofs) left. Although equation (1) represents quite closely the true behaviour of a vibrating structure, it is not directly used in the system identification methods described in this paper. The reasons are the following. Firstly, this equation is in continous time, whereas measurements are mostly sampled at discrete-time instants. Secondly, it is not possible to measure all dofs (as implied by this equation). And finally, there is some noise modelling needed: there may be other unknown excitation sources next to $F(t)$ and measurement noise is always present in real life. Moreover, it is typical for output-only cases that the detailed knowledge of the excitation is replaced by the assumption that the system is excited by white noise. For all these reasons, the equation of dynamic equilibrium (1) will be converted to a more suitable form: the discrete-time stochastic state-space model. The state-space model originates from control theory, but it also appears in mechanical/civil engineering to compute the modal parameters of a dynamic structure with a general viscous damping model (in case of proportional damping one does not need the state-space description to find the modal decomposition) [17].

Following derivations are almost classical and most of them can for instance be found in Juang [18]. With the following definitions,

$$x(t) = \begin{pmatrix} U(t) \\ \dot{U}(t) \end{pmatrix},\ A_c = \begin{pmatrix} 0 & I_{n_2} \\ -M^{-1}K & -M^{-1}C_2 \end{pmatrix},\ B_c = \begin{pmatrix} 0 \\ M^{-1}B_2 \end{pmatrix} \tag{2}$$

equation (1) can be transformed into the state equation

$$\dot{x}(t) = A_cx(t) + B_cu(t) \tag{3}$$

where $A_c \in \mathbb{R}^{n \times n}$ is the state matrix ($n = 2n_2$), $B_c \in \mathbb{R}^{n \times m}$ is the input matrix and $x(t) \in \mathbb{R}^{n \times 1}$ is the state vector. The number of elements of the state-space vector is the number of independent variables needed to describe the state of a system.

In practice, not all the dofs are monitored. If it is assumed that the measurements are evaluated at only l sensor locations, and that these sensors can be accelerometers, velocity or displacement transducers, the observation equation is [18]

$$y(t) = C_a\ddot{U}(t) + C_v\dot{U}(t) + C_dU(t) \tag{4}$$

where $y(t) \in \mathbb{R}^{l \times 1}$ are the outputs, and C_d, C_v, $C_a \in \mathbb{R}^{l \times n_2}$ are the output matrices for displacement, velocity, acceleration. With the following definitions,

$$C = [C_d - C_aM^{-1}K \quad C_v - C_aM^{-1}C_2], \quad D = C_aM^{-1}B_2 \tag{5}$$

equation (4) can be transformed into:

$$y(t) = Cx(t) + Du(t) \tag{6}$$

where $C \in \mathbb{R}^{l \times n}$ is the output matrix and $D \in \mathbb{R}^{l \times m}$ is the direct transmission matrix. In many papers, this direct transmission matrix D is omitted for some reason. However, mostly, accelerations are measured in a practical vibration experiment and since in this case $C_a \neq 0$ (5), D should be part of the state-space model.

Equations (3) and (6) constitute a continuous-time deterministic state-space model. Continuous time means that the expressions can be evaluated at each time instant $t \in \mathbb{R}$ and deterministic means that the input–output quantities $u(t)$, $y(t)$ can be measured exactly. Of course, this is not realistic: measurements are available at discrete time instants $k\Delta t$, $k \in \mathbb{N}$ with Δt, the sample time and noise is always influencing the data. After sampling, the state-space model looks like

$$\begin{aligned} x_{k+1} &= Ax_k + Bu_k \\ y_k &= Cx_k + Du_k \end{aligned} \tag{7}$$

where $x_k = x(k\Delta t)$ is the discrete-time state vector, $A = \exp(A_c \Delta t)$ is the discrete state matrix and $B = [A - I]A_c^{-1}B_c$ is the discrete input matrix. If A_c is not invertible, another expression holds for B [18]. The stochastic components (noise) are included and we obtain the following discrete-time combined deterministic-stochastic state-space model:

$$\begin{aligned} x_{k+1} &= Ax_k + Bu_k + w_k \\ y_k &= Cx_k + Du_k + v_k \end{aligned} \tag{8}$$

where $w_k \in \mathbb{R}^{n \times 1}$ is the process noise due to disturbances and modelling inaccuracies and $v_k \in \mathbb{R}^{l \times 1}$ is the measurement noise due to sensor inaccuracy. They are both unmeasurable vector signals but we assume that they are zero mean, white and with covariance matrices:

$$\boldsymbol{E}\left[\begin{pmatrix} w_p \\ v_p \end{pmatrix}\begin{pmatrix} w_q^T & v_q^T \end{pmatrix}\right] = \begin{pmatrix} Q & S \\ S^T & R \end{pmatrix}\delta_{pq} \tag{9}$$

where $\boldsymbol{E}$ is the expected value operator and δ_{pq} is the Kronecker delta.

Finally, we can concentrate on the practical problem: in the case of ambient vibration testing the input u_k remains unmeasured and it disappears from equation (8). The input is now implicity modelled by the noise terms w_k, v_k. However, the white noise assumptions of these terms cannot be omitted: it is necessary for the proofs of the system identification methods of next sections. The consequence is that if this white noise assumption is violated, for instance if the input contains some dominant frequency components in addition to white noise, these frequency components cannot be separated from the eigenfrequencies of the system and they will appear as poles of the state matrix A.

3. STOCHASTIC STATE-SPACE MODELS

In this section, some important properties of stochastic state-space systems are given. Also some notations are clarified. The stochastic state-space model is defined as equation (8) without u_k terms:

$$\begin{aligned} x_{k+1} &= Ax_k + w_k \\ y_k &= Cx_k + v_k \end{aligned} \tag{10}$$

with w_k, v_k zero mean $\boldsymbol{E}[w_k] = 0$, $\boldsymbol{E}[v_k] = 0$ and with covariance matrices given by (9). Further the stochastic process is assumed to be stationary with zero mean $\boldsymbol{E}[x_k x_k^T] = \Sigma$, $\boldsymbol{E}[x_k] = 0$ where the state covariance matrix Σ is independent of the time k. w_k, v_k are independent of the actual state $\boldsymbol{E}[x_k w_k^T] = 0, \boldsymbol{E}[x_k v_k^T] = 0$. The output covariance matrices are defined as

$$\Lambda_i \equiv \boldsymbol{E}[y_{k+i} \quad y_k^T] \in \mathbb{R}^{l \times l} \tag{11}$$

and finally the next state-output covariance matrix G is defined as

$$G \equiv \boldsymbol{E}[x_{k+1} \quad y_k^T] \in \mathbb{R}^{n \times l}. \tag{12}$$

From these definitions the following properties are easily deduced:

$$\Sigma = A\Sigma A^T + Q$$

$$\Lambda_0 = C\Sigma C^T + R \tag{13}$$

$$G = A\Sigma C^T + S$$

$$\Lambda_i = CA^{i-1}G. \tag{14}$$

Equation (14) is very important and means that the output covariances can be considered as impulse responses of the deterministic linear time-invariant system A, G, C, Λ_0. Therefore, the classical realisation theory applies which goes back to Ho and Kalman [19] and was extended to stochastic systems by Akaike [20] and Aoki [21]. Such a stochastic realisation algorithm will be explained in the next section. Also in mechanical engineering, this observation (14) is used to feed classical algorithms, that normally work with impulse responses, with output covariances instead: polyreference LSCE, ERA, Ibrahim time domain. A paper that is often referred to in this context was written by James *et al.* [22]. This paper contributed to the introduction in the mechanical engineering community of the idea that it is possible to extract modal parameters from systems that are excited by unknown forces. One often mistakenly thinks that the analysis is restricted to operational deflection shapes in these cases.

Before tackling the identification problem, some notations are explained. In the following the reference outputs will play an important role. Typical for ambient testing of large structures is that not all outputs can be measured at once but that they are divided into several set-ups with overlapping sensors. Candidates for the reference outputs are these sensors, common to every set-up because they are placed at optimal locations on the structure, where it is expected that all modes of vibration are present in the measured data. However, additional sensors may be included as references in the identification of one set-up. Assume that the l elements of the outputs are arranged so as to have the r references first; then we have

$$y_k \equiv \begin{pmatrix} y_k^{\text{ref}} \\ y_k^{\sim\text{ref}} \end{pmatrix}, \quad y_k^{\text{ref}} = Ly_k, \quad L \equiv [I_r \; 0] \tag{15}$$

where $y_k^{\text{ref}} \in \mathbb{R}^{r \times 1}$ are the reference outputs and $y_k^{\sim\text{ref}} \in \mathbb{R}^{(l-r) \times 1}$ are the others; $L \in \mathbb{R}^{r \times l}$ is the selection matrix that selects the references. We can now define the covariance matrices between all outputs and the references:

$$\Lambda_i^{\text{ref}} \equiv \boldsymbol{E}[y_{k+i}\, y_k^{\text{ref}^T}] = \Lambda_i L^T \in \mathbb{R}^{l \times r}. \tag{16}$$

For the next state-reference output covariance we have

$$G^{\text{ref}} \equiv \boldsymbol{E}[x_{k+1}\, y_k^{\text{ref}^T}] = GL^T \in \mathbb{R}^{n \times r}. \tag{17}$$

These expressions can be compared with the more classical expressions equations (11) and (12). The important property (14) now reads

$$\Lambda_i^{\text{ref}} = CA^{i-1}G^{\text{ref}}. \tag{18}$$

The output measurements are gathered in a block Hankel matrix with $2i$ block rows and j columns. The first i blocks have r rows, the last i have l rows. For statistical reasons, it is assumed that $j \to \infty$. The Hankel matrix can be divided into a past reference and a future part (a Hankel matrix is a matrix where each antidiagonal consists of the repetition of the same element):

$$H \equiv \frac{1}{\sqrt{j}} \left(\begin{array}{cccc} y_0^{\text{ref}} & y_1^{\text{ref}} & \cdots & y_{j-1}^{\text{ref}} \\ y_1^{\text{ref}} & y_2^{\text{ref}} & \cdots & y_j^{\text{ref}} \\ \cdots & \cdots & \cdots & \cdots \\ y_{i-1}^{\text{ref}} & y_i^{\text{ref}} & \cdots & y_{i+j-2}^{\text{ref}} \\ \hline y_i & y_{i+1} & \cdots & y_{i+j-1} \\ y_{i+1} & y_{i+2} & \cdots & y_{i+j} \\ \cdots & \cdots & \cdots & \cdots \\ y_{2i-1} & y_{2i} & \cdots & y_{2i+j-2} \end{array} \right) \equiv \left(\begin{array}{c} Y_{0|i-1}^{\text{ref}} \\ \hline Y_{i|2i-1} \end{array} \right) \equiv \left(\begin{array}{c} Y_p^{\text{ref}} \\ \hline Y_f \end{array} \right) \begin{array}{l} \updownarrow ri \ \text{“past”} \\ \hline \updownarrow li \ \text{“future”} \end{array} \in \mathbb{R}^{(r+l)i \times j}. \tag{19}$$

Remark that the output data is scaled by a factor $1/\sqrt{j}$. The subscripts of $Y_{i|2i-1} \in \mathbb{R}^{li \times j}$ are the subscript of the first and last element in the first column of the block Hankel matrix. The subscripts p and f stand for past and future. The matrices Y_p^{ref} and Y_f are defined by splitting H into two parts of i block rows. Another division is obtained by adding one block row to the past references and omitting the first block row of the future outputs. Because the references are only a subset of the outputs ($r \leqslant l$), $l - r$ rows are left over in this new division. These rows are denoted by $Y_{i|i}^{\sim\text{ref}} \in \mathbb{R}^{(l-r)\times j}$:

$$H = \left(\begin{array}{c} Y_{0|i}^{\text{ref}} \\ \hline Y_{i|i}^{\sim\text{ref}} \\ \hline Y_{i+1|2i-1} \end{array} \right) = \left(\begin{array}{c} Y_p^{\text{ref}+} \\ \hline Y_{i|i}^{\sim\text{ref}} \\ \hline Y_f^- \end{array} \right) \begin{array}{l} \updownarrow r(i+1) \\ \hline \updownarrow l - r \\ \hline \updownarrow l(i-1) \end{array} \tag{20}$$

Some other matrices need to be defined. The extended observability matrix is

$$O_i \equiv \left(\begin{array}{c} C \\ CA \\ CA^2 \\ \cdots \\ CA^{i-1} \end{array} \right) \in \mathbb{R}^{li \times n} \tag{21}$$

The matrix pair $\{A, C\}$ is assumed to be observable, which implies that all the dynamical modes of the system can be observed in the output. The reference reversed extended stochastic controllability matrix is defined as

$$C_i^{\text{ref}} \equiv (A^{i-1}G^{\text{ref}} \quad A^{i-2}G^{\text{ref}} \cdots AG^{\text{ref}} \quad G^{\text{ref}}) \in \mathbb{R}^{n \times ri} \tag{22}$$

The matrix pair $\{A, G^{\text{ref}}\}$ is assumed to be controllable, which implies that all the dynamical modes of the system can be excited by the stochastic input.

4. REFERENCE-BASED COVARIANCE-DRIVEN STOCHASTIC REALISATION

In this section, a modified version of the classical covariance-driven stochastic realisation algorithm [7, 20, 21] is presented. The modification consists of reformulating the algorithm so that it only needs the covariances between the outputs and a limited set of reference outputs instead of the covariances between all outputs [22, 23]. The background of this algorithm helps to understand the reference-based stochastic subspace algorithm presented in the next section that makes use of the output data directly without the need to estimate the output covariances. The covariance matrices between all outputs and a set of references have already been defined in equation (16) as $\Lambda_i^{\text{ref}} \equiv \boldsymbol{E}[y_{k+i}\, y_k^{\text{ref}^T}]$. They are gathered in a block Toeplitz matrix (a Toeplitz matrix is a matrix where each diagonal consists of the repetition of the same element):

$$T_{1|i}^{\text{ref}} \equiv \begin{pmatrix} \Lambda_i^{\text{ref}} & \Lambda_{i-1}^{\text{ref}} & \cdots & \Lambda_1^{\text{ref}} \\ \Lambda_{i+1}^{\text{ref}} & \Lambda_i^{\text{ref}} & \cdots & \Lambda_2^{\text{ref}} \\ \cdots & \cdots & \cdots & \cdots \\ \Lambda_{2i-1}^{\text{ref}} & \Lambda_{2i-2}^{\text{ref}} & \cdots & \Lambda_i^{\text{ref}} \end{pmatrix} \in \mathbb{R}^{li \times ri}. \tag{23}$$

From equation (19) and assuming ergodicity, the block Toeplitz matrix equals

$$T_{1|i}^{\text{ref}} = Y_f Y_p^{\text{ref}^T}. \tag{24}$$

Because equation (18) the block Toeplitz matrix decomposes as

$$T_{1|i}^{\text{ref}} = \begin{pmatrix} C \\ CA \\ \cdots \\ CA^{i-1} \end{pmatrix} (A^{i-1}G^{\text{ref}}\, A^{i-2}G^{\text{ref}} \ldots AG^{\text{ref}}\, G^{\text{ref}}) = O_i C_i^{\text{ref}}. \tag{25}$$

Both factors, the observability and reference-reversed controllability matrix, can be obtained by applying the singular-value decomposition (SVD) to the block Toeplitz matrix:

$$T_{1|i}^{\text{ref}} = USV^T = (U_1\ U_2)\begin{pmatrix} S_1 & 0 \\ 0 & 0 \end{pmatrix}\begin{pmatrix} V_1^T \\ V_2^T \end{pmatrix} = U_1 S_1 V_1^T \tag{26}$$

where $U \in \mathbb{R}^{li \times li}$ and $V \in \mathbb{R}^{ri \times ri}$ are orthonormal matrices $U^TU = UU^T = I_{li}$ and $V^TV = VV^T = I_{ri}$ and $S \in \mathbb{R}^{li \times ri}$ is a diagonal matrix containing the singular values in descending order. Since the inner dimension of the product $O_i C_i^{\text{ref}}$ equals n and since we assume that $ri \geqslant n$, the rank of the product cannot exceed n. The rank of a matrix is found as the number of non-zero singular values. In the last equality of equation (26), the zero singular values and corresponding singular vectors are omitted. With equations (25) and (26), we can now state that

$$\begin{aligned} O_i &= U_1 S_1^{1/2} \\ C_i^{\text{ref}} &= S_1^{1/2} V_1^T. \end{aligned} \tag{27}$$

Once O_i and C_i^{ref} are known, the solution to the identification problem is straightforward. From equations (21) and (22) we know that C equals the first l rows of O_i and G^{ref} equals the

last r columns of C_i^{ref}. The state matrix A can, for instance, be found by decomposing a shifted block Toeplitz matrix:

$$T_{2|i+1}^{\text{ref}} = O_i A C_i^{\text{ref}} \tag{28}$$

and solving equation (28) for A by introducing equation (27):

$$A = O_i^{\dagger} T_{2|i+1}^{\text{ref}} C_i^{\text{ref}\dagger} = S_i^{-1/2} U_1^T T_{2|i+1}^{\text{ref}} V_1 S_1^{-1/2} \tag{29}$$

where $(\bullet)^{\dagger}$ represents the pseudo-inverse of a matrix.

At this point the identification problem is theoretically solved: based on the output covariances the system order n and the system matrices A, G^{ref}, C are recovered. A first comment that can be made when applying the covariance-driven stochastic realisation algorithm to measurements is that in reality the number of measurements is not infinite, $j \neq \infty$, and therefore the covariances computed by equation (24) are not the true covariances but only estimates. Another remark is that in theory the system order n can be determined by inspecting the number of non-zero singular values of $T_{1|i}^{\text{ref}}$ in equation (26). In practice, however, due to noise (modelling inaccuracies, measurement noise and computational noise) the higher singular values are not exactly zero. In this case, the order can be determined by looking at a 'gap' between two successive singular values. The singular value where the maximal gap occurs yields the model order. This criterion should however not be applied dogmatically. For large, real structures there is generally no clear gap.

5. REFERENCE-BASED DATA-DRIVEN STOCHASTIC SUBSPACE

In this section, a novel reference-based version of the stochastic identification (SSI) method is presented. The key step of SSI is the projection of the row space of the future outputs into the row space of the past outputs [24]. The idea is now to take instead of all past outputs only the past reference outputs. This reduces the dimensions of the problem and thus also the computation time. In modal analysis applications, often, a lot of sensors are used. They have a certain spatial distribution over the structure, leading to signals of different quality. Some sensors are located at nodal points of a mode shape and others may be located at points close to fixed boundaries: e.g. for most civil engineering structures it is generally impossible to obtain a free–free set-up. Since the number of references is limited, their quality is important: all modes must be present in the data measured by the references. If the 'best' sensors are selected as references, no loss of identification quality is expected. On the contrary, because the lower quality sensors are partially omitted, the identification results may be more accurate. The reason why the projection is not limited to the reference future outputs too, is that in this case one would obtain mode shapes amplitudes at the reference sensors only, whereas one is interested in the mode shapes at all measured locations. The new algorithm is denoted as SSI/ref: reference-based stochastic subspace identification.

The comparison between the covariance-driven stochastic realisation algorithm (Section 4) and the data-driven stochastic subspace algorithm (Section 5) is made in a separate Section (Section 6).

5.1. KALMAN FILTER STATES

The Kalman filter states play an important role in stochastic subspace identification. The meaning of Kalman filter states will briefly be explained. More details can be found in the literature [3, 18, 24]. The aim of the Kalman filter is to produce an optimal prediction for

the state vector x_{k+1} by making use of observations of the outputs up to time k and the available system matrices together with the known noise covariances. These optimal predictions are denoted by a hat ($\hat{x}_{k+1}$). When the initial state estimate ($\hat{x}_0 = 0$), the initial covariance of the state estimate ($P_0 \equiv \boldsymbol{E}[\hat{x}_0 \hat{x}_0^T] = 0$) and the output measurements ($y_0, \ldots, y_k$) are given, the non-steady-state Kalman filter state estimates $\hat{x}_{k+1}$ are defined by the following recursive formulas, expressing the system, the Kalman filter gain matrix and the state covariance matrix:

$$\begin{aligned} \hat{x}_{k+1} &= A\hat{x}_k + K_k(y_k - C\hat{x}_k) \\ K_k &= (G - AP_kC^T)(\Lambda_0 - CP_kC^T)^{-1} \\ P_{k+1} &= AP_kA^T + (G - AP_kC^T)(\Lambda_0 - CP_kC^T)^{-1}(G - AP_kC^T)^T. \end{aligned} \tag{30}$$

The Kalman filter state estimates are gathered to form the Kalman filter state sequence, that will be recovered by the stochastic subspace algorithm (see further):

$$\hat{X}_i \equiv (\hat{x}_i \ \hat{x}_{i+1} \ \ldots \ \hat{x}_{i+j-1}) \in \mathbb{R}^{n \times j}. \tag{31}$$

5.2. PROJECTIONS

First we take the QR-factorisation of the block Hankel matrix (19) consisting of past references and future outputs:

$$H \equiv \begin{pmatrix} Y_p^{\text{ref}} \\ \hline Y_f \end{pmatrix} = RQ^T \tag{32}$$

where $Q \in \mathbb{R}^{j \times j}$ is an orthonormal matrix $Q^TQ = QQ^T = I_j$ and $R \in \mathbb{R}^{(r+l)i \times j}$ is a lower triangular matrix. Since $(r + l)i < j$ we can omit the zeros in R and the corresponding zeros of Q:

$$H = \begin{array}{c} \begin{array}{cccccc} & ri & r & l-r & l(i-1) & j \to \infty \\ & \leftrightarrow & \leftrightarrow & \leftrightarrow & \leftrightarrow & \leftrightarrow \end{array} \\ \begin{array}{c} ri \\ r \\ l-r \\ l(i-1) \end{array} \begin{pmatrix} R_{11} & 0 & 0 & 0 \\ R_{21} & R_{22} & 0 & 0 \\ R_{31} & R_{32} & R_{33} & 0 \\ R_{41} & R_{42} & R_{43} & R_{44} \end{pmatrix} \end{array} \begin{pmatrix} Q_1^T \\ Q_2^T \\ Q_3^T \\ Q_4^T \end{pmatrix} \begin{array}{c} \updownarrow \\ \updownarrow \\ \updownarrow \\ \updownarrow \end{array} \begin{array}{c} ri \\ r \\ l-r \\ l(i-1) \end{array} \tag{33}$$

Further in the algorithm, the Q-factors will cancel out because of their orthonormality. So we do not need them and we achieved an important data reduction. As stated before, projections are important in subspace identification. The projection of the row space of the future outputs into the row space of the past reference outputs is defined as

$$\mathscr{P}_i^{\text{ref}} \equiv Y_f / \mathbf{Y}_{\text{p}}^{\text{ref}} \equiv Y_f Y_p^{\text{ref}^T} (Y_p^{\text{ref}} Y_p^{\text{ref}^T})^{\dagger} Y_p^{\text{ref}}. \tag{34}$$

The idea behind this projection is that it retains all the information in the past that is useful to predict the future. Introducing the QR-factorisation of the output Hankel matrix (33) into equation (34) gives the following simple expression for the projection:

$$\mathscr{P}_i^{\text{ref}} = \begin{pmatrix} R_{21} \\ R_{31} \\ R_{41} \end{pmatrix} Q_1^T \in \mathbb{R}^{li \times j}. \tag{35}$$

The main theorem of stochastic subspace identification [24] states that the projection $\mathscr{P}_i^{\text{ref}}$ can be factorised as the product of the observability matrix (21) and the Kalman filter state sequence (31):

$$\mathscr{P}_i^{\text{ref}} = \begin{pmatrix} C \\ CA \\ CA^2 \\ \cdots \\ CA^{i-1} \end{pmatrix} (\hat{x}_i \quad \hat{x}_{i+1} \quad \cdots \quad \hat{x}_{i+j-1}) \equiv O_i \hat{X}_i. \tag{36}$$

Remember that this formula holds asymptotically only for $j \to \infty$. The proof of this theorem for algorithms where all past outputs have been used (SSI) can be found in Van Overschee and De Moor [24]. In the present case, where only the past reference outputs have been used (SSI/ref), the proof is almost the same, except for the significance of the obtained Kalman filter state sequence $\hat{X}_i$. The Kalman state estimate is in this case the optimal prediction for the states by making use of observations of the reference outputs only instead of all outputs as in Section 5.1. At first sight there seems to be no difference between SSI and SSI/ref: in both cases the same decomposition is found (36). Indeed, theoretically the internal state of a system does not depend on the choice and number of observed outputs. However, in identification problems where the system is estimated based on observations, the choice and number of outputs does matter. The Kalman filter state estimates in SSI/ref will differ from the SSI-estimates.

Both factors of equation (36), the observability matrix O_i and the state sequence $\hat{X}_i$ are obtained by applying the SVD to the projection matrix:

$$\mathscr{P}_i^{\text{ref}} = U_1 S_1 V_1^T. \tag{37}$$

Since $rank(\mathscr{P}_i^{\text{ref}}) = n$, we have $U_1 \in \mathbb{R}^{li \times n}$, $S_1 \in \mathbb{R}^{n \times n}$, $V_1 \in \mathbb{R}^{j \times n}$. Combining equations (36) and (37) gives

$$O_i = U_1 S_1^{1/2}, \qquad \hat{X}_i = O_i^{\dagger} \mathscr{P}_i^{\text{ref}}. \tag{38}$$

5.3. DETERMINATION OF THE SYSTEM MATRICES

Up to now we found the order of the system n (as the number of non-zero singular values in equation (37)), the observability matrix O_i and the state sequence $\hat{X}_i$. This section explains how to recover the system matrices A, C, Q, R, S. Using the shifted past and future outputs of the data Hankel matrix (20) another projection is obtained:

$$\mathscr{P}_{i-1}^{\text{ref}} \equiv Y_f^- / \mathbf{Y}_p^{\text{ref}+} = (R_{41} \;\; R_{42}) \begin{pmatrix} Q_1^T \\ Q_2^T \end{pmatrix} \in \mathbb{R}^{l(i-1) \times j}. \tag{39}$$

The first equality defines the projection, the second explains how to compute it from equation (33). It can be proved similar to equation (36) that

$$\mathscr{P}_{i-1}^{\text{ref}} = O_{i-1} \hat{X}_{i+1}. \tag{40}$$

O_{i-1} is obtained after deleting the last l rows of O_i computed as in equation (38). The shifted state sequence is now obtained as

$$\hat{X}_{i+1} = O_{i-1}^{\dagger} \mathscr{P}_{i-1}^{\text{ref}}. \tag{41}$$

At this moment, the Kalman state sequence $\hat{X}_i$, $\hat{X}_{i+1}$ are calculated using only the output data (38), (41). The system matrices can now be recovered from following overdetermined set of linear equations, obtained by extending equation (10):

$$\begin{pmatrix} \hat{X}_{i+1} \\ Y_{i|i} \end{pmatrix} = \begin{pmatrix} A \\ C \end{pmatrix} (\hat{X}_i) + \begin{pmatrix} \rho_w \\ \rho_v \end{pmatrix} \tag{42}$$

where $Y_{i|i}$ is a Hankel matrix with only one block row (19). In order to fit in the QR-scheme, it is written as (33)

$$Y_{i|i} = \begin{pmatrix} R_{21} & R_{22} & 0 \\ R_{31} & R_{32} & R_{33} \end{pmatrix} \begin{pmatrix} Q_1^T \\ Q_2^T \\ Q_3^T \end{pmatrix} \in \mathbb{R}^{l \times j}. \tag{43}$$

Since the Kalman state sequences and the outputs are known and the residuals $(\rho_w^T \ \rho_v^T)^T$ are uncorrelated with $\hat{X}_i$, the set of equations can be solved for A, C in a least-squares sense:

$$\begin{pmatrix} A \\ C \end{pmatrix} = \begin{pmatrix} \hat{X}_{i+1} \\ Y_{i|i} \end{pmatrix} \hat{X}_i^{\dagger} \tag{44}$$

When introducing equations (38), (35), (41), (39) into (44), it is clear that the Q-factors cancel out.

Finally, the noise covariances Q, R, S are recovered as the covariances of the residuals in equation (42). This guarantees the positive realness of the identified covariance sequence [24]. We will come back to the issue of positive realness (Sections 7.2–7.3).

A, C, Q, R, S can be transformed into A, G, C, Λ_0 by solving the Lyapunov equation for Σ (13):

$$\Sigma = A\Sigma A^T + Q \tag{45}$$

after which G and Λ_0 can be computed from (13)

$$\Lambda_0 = C\Sigma C^T + R, \qquad G = A\Sigma C^T + S. \tag{46}$$

At this point the identification problem is theoretically solved: based on the outputs, the system order n and the system matrices A, G, C, Λ_0 were found.

The same remark as with the covariance-based algorithm concerning the determination of the model order n applies. Due to noise (modelling inaccuracies, measurement noise and computational noise) the higher singular values are not exactly zero and the order can only be determined by looking at a 'gap' between two successive singular values. The singular value where the maximal gap occurs yields the model order. However, in many practical cases, no gap is visible. The application will show that the problem of order determination can be solved by constructing the so-called stabilisation diagram (Section 8.3). Another remark is that by imposing positive realness of the identified covariance sequence, a small bias was introduced on the estimates of G and Λ_0.

6. COVARIANCE-DRIVEN VS DATA-DRIVEN SUBSPACE

This section points out some of the similarities and differences between the covariance-driven approach (Section 4) and the data-driven approach (Section 5). First the similarities.

Both methods start with a data-reduction step. In the realisation algorithm, the raw time histories of the data Hankel matrix (19) are converted to the covariances of the Toeplitz matrix (24): $T_{l|i}^{\text{ref}} = Y_f Y_p^{\text{ref}T}$. The number of elements is reduced from $(r+l)i \times j$ to $li \times ri$ (remember that j goes to infinity). In the subspace algorithm, a similar reduction is obtained by projecting the row space of the future outputs into the row space of the past reference outputs (34): $\mathscr{P}_i^{\text{ref}} \equiv Y_f / \mathbf{Y}_p^{\text{ref}}$. This projection is computed using the QR-factorisation of the data Hankel matrix (33). A significant data reduction is obtained because only the R-factor is further needed in the algorithm. Both methods then proceed with a singular-value decomposition. The decomposition of $T_{1|i}^{\text{ref}}$ reveals the order of the system, the column space of O_i and the row space of C_i^{ref} (25–27). Similarly, the decomposition of $\mathscr{P}_i^{\text{ref}}$ reveals the order of the system, the column space of O_i and the row space of $\hat{X}_i$ (36–38). In [24] it is shown that by an appropriate weighting of $\mathscr{P}_i$ (all outputs are considered in [24]: $\mathscr{P}_i^{\text{ref}} \to \mathscr{P}_i$), the covariance-driven algorithms available in literature can be fitted into the framework of the data-driven subspace methods. This completes the similarities.

Equation (24) is one way of estimating the output covariances, but not the fastest one. Note that it is indeed an estimate since in reality $j \neq \infty$. Another possibility is computing the covariances as the inverse discrete Fourier transform of the auto- and cross-spectra of the outputs. The spectra can be estimated by applying the discrete Fourier transform to the output time histories. This second possibility is considerably faster but less accurate due to leakage errors. Anyhow the use of Fourier transforms makes the covariance-driven methods less time-consuming than the data-driven methods which imply a slower QR-factorisation step.

An advantage of the data-driven method is that it is implemented as a numerically robust square root algorithm: the matrices are not squared up as in the covariance-driven algorithm (24). More advantages of the data-driven method become clear in Sections 7.2 and 7.3 where some validation tools for the identified state-space model are presented: an expression of the spectra based on the identified state-space matrices and the separation of the total response in modal contributions.

7. POSTPROCESSING

7.1. MODAL ANALYSIS

This section explains how the system identification results of previous section can be used in modal analysis of structures. System identification [3] is the general term that stands for experiment-based modelling of 'systems': biological, chemical, economical, industrial, climatological, mechanical, etc. The system is subjected to an input and the responses are measured. After adopting a certain model for the system, values are assigned to the model parameters so that the model matches the measured data. In the previous sections, a stochastic state-space model was identified using output data. Modal analysis can be considered as a particular type of system identification: instead of describing the system by means of rather abstract mathematical parameters, the system's behaviour is now expressed in terms of its modes of vibration. A mode is characterised by an eigenfrequency, a damping ratio, a mode shape and a modal scaling factor. Note that in output-only modal analysis, this last parameter cannot be estimated.

As a result of the identification the discrete state matrix A is obtained. The dynamic behaviour of the system is completely characterised by its eigenvalues:

$$A = \Psi \Lambda \Psi^{-1} \tag{47}$$

where $\Lambda = diag(\lambda_q) \in \mathbb{C}^{n\times n}$, $q = 1, \ldots, n$, is a diagonal matrix containing the discrete-time complex eigenvalues and $\Psi \in \mathbb{C}^{n\times n}$ contains the eigenvectors as columns. The continuous-time state equation (3) is equivalent to the second-order matrix equation of motion (1). Consequently, they have the same eigenvalues and eigenvectors. These can be obtained by an eigenvalue decomposition of the continuous-time state matrix:

$$A_c = \Psi_c \Lambda_c \Psi_c^{-1} \tag{48}$$

where $\Lambda_c = diag(\lambda_{c_q}) \in \mathbb{C}^{n\times n}$ is a diagonal matrix containing the continuous-time complex eigenvalues and $\Psi_c \in \mathbb{C}^{n\times n}$ contains the eigenvectors as columns. Because of relation (7),

$$A = \exp(A_c \Delta t). \tag{49}$$

we have

$$\Psi_c = \Psi, \lambda_{c_q} = \frac{\ln(\lambda_q)}{\Delta t}. \tag{50}$$

The eigenvalues of A_c occur in complex conjugated pairs and can be written as

$$\lambda_{c_q}, \lambda_{c_q}^* = -\xi_q \omega_q \pm j\omega_q \sqrt{1-\xi_q^2} \tag{51}$$

where ξ_q is the modal damping ratio of mode q and ω_q is the eigenfrequency of mode q (rad/s).

The estimated states of the system x_k do not necessarily have a physical meaning. Therefore, the eigenvectors of the state matrix Ψ need to be transferred to the outside world. The mode shapes at the sensor locations, defined as columns Φ_q of $\Phi \in \mathbb{C}^{l\times n}$, are the observed parts of the system eigenvectors Ψ and are thus obtained using the observation equation (6):

$$\Phi = C\Psi. \tag{52}$$

In this section, it was shown how the modal parameters ω_q, ξ_q, Φ_q can be extracted analytically from the identified system matrices A, C.

7.2. SPECTRUM ANALYSIS

It is also possible to derive an analytical expression for the spectrum based on the identified stochastic state-space matrices A, G, C, Λ_0. In Caines [25], it is shown that the spectrum of a stochastic system can be written as

$$S_{yy}(z) = [C(zI_n - A)^{-1}G + \Lambda_0 + G^T(z^{-1}I_n - A^T)^{-1}C^T]_{z=e^{j\omega\Delta t}} \tag{53}$$

where $S_{yy}(z) \in \mathbb{C}^{l\times l}$ is the spectrum matrix containing the auto- and cross-spectra between the outputs. The autospectra are real and located on the main diagonal. This expression (53) can be evaluated for any number on the unit circle $z = e^{j\omega\Delta t}$ where ω (rad/s) can be any frequency of interest. For the implementation of the reference-based stochastic realization algorithm presented in Section 4, the complete analytical spectrum matrix (53) does not exist. Only the auto- and cross-spectra between the reference outputs can be determined, since it is not $G \in \mathbb{R}^{n\times l}$ (12) but only $G^{\text{ref}} \in \mathbb{R}^{n\times r}$ (17) which is identified. Also this algorithm does not guarantee positive realness of the identified covariance sequence Λ_i(11). One of the consequences is that the Z-transform of this sequence, which is the spectrum (53), is not a positive-definite matrix for all $z = e^{j\omega\Delta t}$ on the unit circle [24]. In other words, the analytical spectrum can become negative which has of course no physical meaning. The implementation of SSI and SSI/ref presented in Section 5 does not suffer from these two shortcomings.

7.3. MODAL RESPONSE AND PREDICTION ERRORS

It can be shown that the stochastic state-space model (10) can be converted to a forward innovation form by solving a Riccati equation:

$$\begin{aligned} z_{k+1} &= Az_k + Ke_k \\ y_k &= Cz_k + e_k \end{aligned} \tag{54}$$

where $K \in \mathbb{R}^{n \times l}$ is the Kalman gain and $e_k \in \mathbb{R}^{l \times 1}$ are the innovations with covariance matrix $E[e_p e_q^T] = R_e \delta_{pq}$. Note that the state vector z_k is different from x_k because of the different state space basis. With equations (47) and (52) this model can be written in the modal basis:

$$\begin{aligned} z_{m_{k+1}} &= \Lambda z_{m_k} + K_m e_k \\ y_k &= \Phi z_{m_k} + e_k \end{aligned} \tag{55}$$

where $\Psi^{-1} z_k = z_{m_k}$, $\Psi^{-1} K = K_m$. By eliminating the innovations in the first equation we obtain

$$\begin{aligned} z_{m_{k+1}} &= (\Lambda - K_m \Phi) z_{m_k} + K_m y_k \\ \hat{y}_k &= \Phi z_{m_k} \end{aligned} \tag{56}$$

where $\hat{y}_k$ is the one-step-ahead predicted output and the innovations are the prediction errors $e_k = y_k - \hat{y}_k$. The state-space model $(\Lambda - K_m \Phi, K_m, \Phi, 0)$ (56) can be simulated with the measured outputs y_k serving as inputs. As the outcome of the simulation we get the states in modal basis z_{m_k} and the predicted outputs $\hat{y}_k$. Since Λ (55) is a diagonal matrix, the contribution of each mode to the total response can be separated. If $(z_{m_k})_q$ represents component q of z_{m_k}, the modal response of mode q is defined as

$$\hat{y}_k^{(q)} = \Phi_q (z_{m_k})_q. \tag{57}$$

The total measured response can be decomposed as

$$y_k = \sum_{q=1}^{n} \Phi_q (z_{m_k})_q + e_k. \tag{58}$$

The simulation (56) not only yields the prediction errors but also the modal contributions to the total response. Note that for obtaining the prediction errors it was not necessary to convert the state space to the modal basis. They could also be computed from equation (54).

Note that the approach of this section is only possible in combination with the data-driven subspace method. In order to obtain the forward innovation form (54), the full G matrix is needed and not only G^{ref} as obtained in the covariance-driven method. Moreover the covariance-driven implementation does not guarantee a positive real covariance sequence which means that it is not always possible to obtain a forward innovation model [24].

8. APPLICATION: STEEL MAST EXCITED BY WIND

8.1. INTRODUCTION

In the design process of a steel transmitter mast, the damping ratios of the lower modes are important factors. The wind turbulence spectrum has a peak value at a very low

frequency of about 0.04 Hz [26]. All eigenfrequencies of the considered structure are situated at the descending part of the turbulence power spectrum, and thus in fact only the few lower modes of vibration are important for determining the structure's response to dynamic wind load. The structure under consideration is a steel frame structure with antennae attached at the top. In order to prevent malfunctioning of the antennae, the rotation at the top has to be limited to 1°. Only once in 10 years, this value may be exceeded. The dynamic response (and thus the rotation angle) of a structure reaches its maximum at resonance, where the amplitude is inversely proportional to the damping ratio. So the damping is directly related to the maximum rotation angle. A high damping ratio means that the amount of steel needed to meet the specification of limited rotation can be reduced. Therefore, a vibration experiment was performed on a steel transmitter mast in order to determine these damping ratios. Since it is very difficult, if not impossible, to measure the dynamic wind load, only response measurements were recorded and the mast constitutes an excellent real-life example to validate output-only system identification methods.

8.2. STRUCTURE AND DATA ACQUISITION

Figure 1 gives a general view of the structure. A typical cross-section is illustrated in Fig. 2. The mast has a triangular cross-section consisting of three circular hollow section profiles. The three main tubes are connected to smaller tubes forming the diagonal and horizontal members of the truss structure. The structure is composed of five segments of 6 m, reaching a height of 30 m. At the top in the centroid of the section, an additional tube rises above the truss structure resulting in a total height of 38 m. A ladder is attached to one side of the triangle. Together with the diagonals, this ladder disturbs, somewhat, the symmetry of the structure. Further, the mast is founded on a thick concrete slab supported by three piles. A first test was carried out on 24 February 1997 [27]. The obtained damping ratios were very low: 0.2–0.5%. However at that time the transmitter equipment (the antennae) was not yet placed. Therefore, a new test was performed on 26 March 1998. The sectorial antennae for a cellular phone network, situated at a height of about 33 m (Fig. 1), are expected to have an important influence on the dynamics of the structure. The additional mass (+ 10%) is considerable and it is located at a place where large displacements occur.

The measurement grid for the dynamic test consisted of 23 points: every 6 m, from 0 to 30 m, three horizontal accelerations were measured. Their measurement direction is denoted in Fig. 2 by H1, H2, H3. Assuming that the triangular cross-section remains undeformed during the test, the three measured accelerations are sufficient to describe the complete horizontal movement of the considered section. At ground level (0 m) also three vertical accelerations were measured in order to have a complete description of all displacement components of the foundation. Another difference as opposed to the first test was that two supplementary sensors were installed on the central tube at 33 m. These two sensors measuring in both horizontal directions allow a better characterisation of the mode shapes. Due to the limited number of acquisition channels and high-sensitivity accelerometers, the measurement grid of 23 sensor positions was split into four set-ups. In output-only modal analysis where the input force remains unknown and may vary between the set-ups, the different measurement set-ups can only be linked if there are some sensors in common. The three sensors at 30 m are suitable as references since it is not expected that these are situated at a node of any mode shape. The cut-off frequency of the anti-aliasing filter was set at 20 Hz. The data were sampled at 100 Hz. A total of 30 720 samples was acquired for each channel, resulting in a measurement time of about 5 min for each set-up. In Fig. 3, a typical time signal and its power spectrum is represented.

Figure 1. Steel transmitter mast with eccentric antennae at the top.

8.3. SYSTEM IDENTIFICATION

Before identification the data was decimated with factor 8: it was filtered through a digital low-pass filter with a cut-off frequency of 5 Hz and resampled at 12.5 Hz. This operation reduces the number of data points to 3840 and makes the identification more accurate in the considered frequency range 0–5 Hz. There are nine outputs l of which the first 3 are considered as references r. The number of block rows i (19) is taken as 10, resulting in a maximal model order of $ri = 30$ in SSI/ref and $li = 90$ in SSI, if all singular values are retained (37).

There exist several implementations of the stochastic subspace method [24]; one of these is the canonical variate algorithm (CVA). In this algorithm, the singular values can be interpreted as the cosines of the principal angles between two subspaces: the row space of

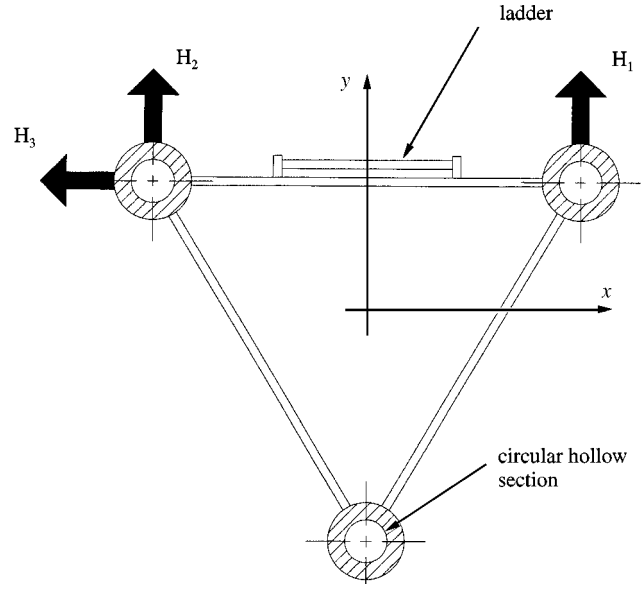

Figure 2. Typical cross-section of mast.

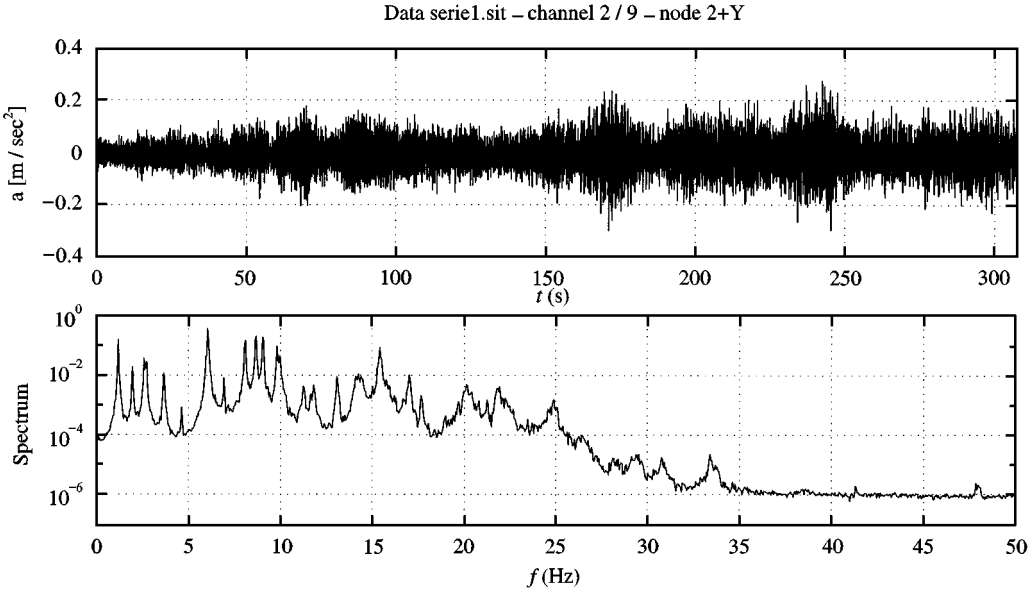

Figure 3. Horizontal acceleration measured at 30 m. (top) Time signal, (bottom) power spectrum.

the past (reference) outputs and the future outputs. Figure 4 represents these principal angles for both SSI/ref and SSI. As explained in Section 5.3 the true model order is found by looking for a gap in the principal angles. The gap for SSI/ref is located at $n = 14$ and for SSI at $n = 18$. The graph suggests that SSI/ref: requires a lower model order to fit the data.

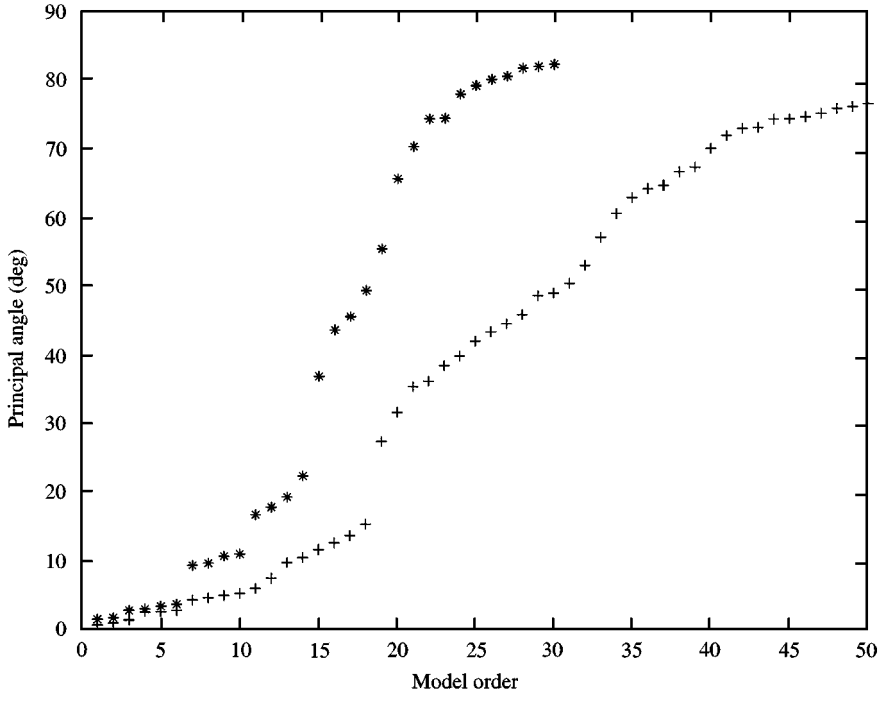

Figure 4. Principal angles between two subspaces computed for both subspace methods. $*$, SSI/ref; $+$, SSI.

There are two possible explanations: an unfavourable and a favourable one to SSI/ref: the method is not able to extract all useful information from the data or it gets rid of the noise faster because the reference outputs have the highest signal-to-noise ratios. It will be demonstrated that the second explanation is more likely.

In modal analysis applications, one is not interested in a state-space model that fits the data as such, but rather in the modal parameters that can be extracted from that model (47). Practical experience with real data [5, 16, 27] showed that it is better to overspecify the model order and to eliminate spurious numerical poles afterwards. This can be done by constructing stabilisation diagrams. By rejecting less singular values (principal angles), models of increasing order are determined. Each model yields a set of modal parameters and these can be plotted in a stabilisation diagram. In Fig. 5 the diagrams for SSI/ref and SSI are represented. The criteria are 1% for eigenfrequencies, 5% for damping ratios and 1% for mode shape vectors (MAC). Physical poles will show up as stable ones whereas numerical poles will not become stable with increasing order. These diagrams indicate that SSI/ref yields stable poles at a lower order.

If we would zoom around 1.17 Hz in Fig. 5, two stable poles would become visible. So, if the poles around 5 Hz are not counted because they originate from the applied digital low-pass filter, there are seven physical poles present in the data, occurring in complex conjugated pairs. This means that SSI/ref indeed predicted the true model order $n = 14$ (Fig. 4). It must be noted that this rarely happens. In the present case, the response was linear and the signal-to-noise ratio very good, thanks to the well-defined boundary conditions and the flexibility of the structure. This resulted in high-quality signals with clear peaks in the power spectra.

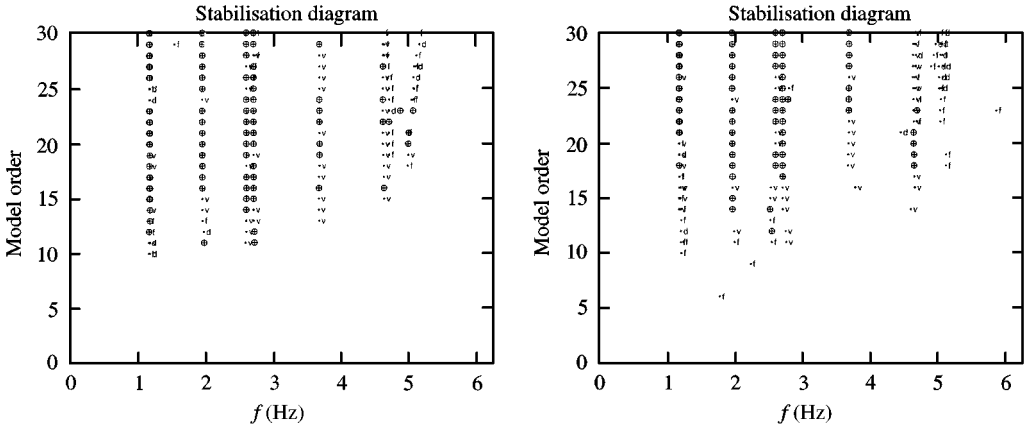

Figure 5. Stabilisation diagrams. The criteria are: 1% for frequencies, 5% for damping ratios, 1% for mode shape vectors (MAC). (left) SSI/ref, (right) SSI. ⊕, stable pole; .v, stable frequency and vector: .d, stable frequency and damping; .f, stable frequency.

TABLE 1

Estimated eigenfrequencies and damping ratios: averge f, ξ and standard deviations σ_f, σ_ξ based on eight samples of SSI/ref and SSI results

Mode no.	Eigenfrequencies				Damping ratios			
	SSI/ref		SSI		SSI/ref		SSI	
	f(Hz)	σ_f(Hz)	f(Hz)	σ_f(Hz)	ξ(%)	σ_ξ(%)	ξ(%)	σ_ξ(%)
1	1.170	0.002	1.171	0.002	0.5	0.2	0.5	0.2
2	1.179	0.001	1.179	0.002	0.7	0.2	0.8	0.2
3	1.953	0.004	1.953	0.004	0.7	0.1	0.7	0.1
4	2.601	0.002	2.601	0.003	0.3	0.1	0.4	0.1
5	2.711	0.001	2.711	0.001	0.17	0.05	0.17	0.04
6	3.687	0.003	3.648	0.002	0.2	0.1	0.3	0.1
7	4.628	0.004	4.633	0.003	0.2	0.1	0.3	0.1

8.4. IDENTIFICATION RESULTS

Rather than trying to find one order and related state-space model where all modes are stable, different orders are selected to determine the modal parameters. There are four set-ups and every set-up was measured twice. So, there are eight estimates for every eigenfrequency and damping ratio. The mean values and standard deviations are represented in Table 1. Unfortunately, there is no statistical information present for mode shapes since four set-ups yield only 1 mode shape estimate. The uncertainties on the eigenfrequencies are extremely low. As usual, the damping ratios are more uncertain. However, it seems that placing the antennae at the top had a positive influence on the damping ratios in the sense that they are somewhat higher for the lowest modes: 0.3–0.7% instead of 0.2–0.5% [27].

From Table 1 there can be hardly seen any difference between the SSI/ref and SSI estimates. By using only the past references, no loss of quality occurred, but there was an important gain concerning computational efficiency: the results were obtained using only

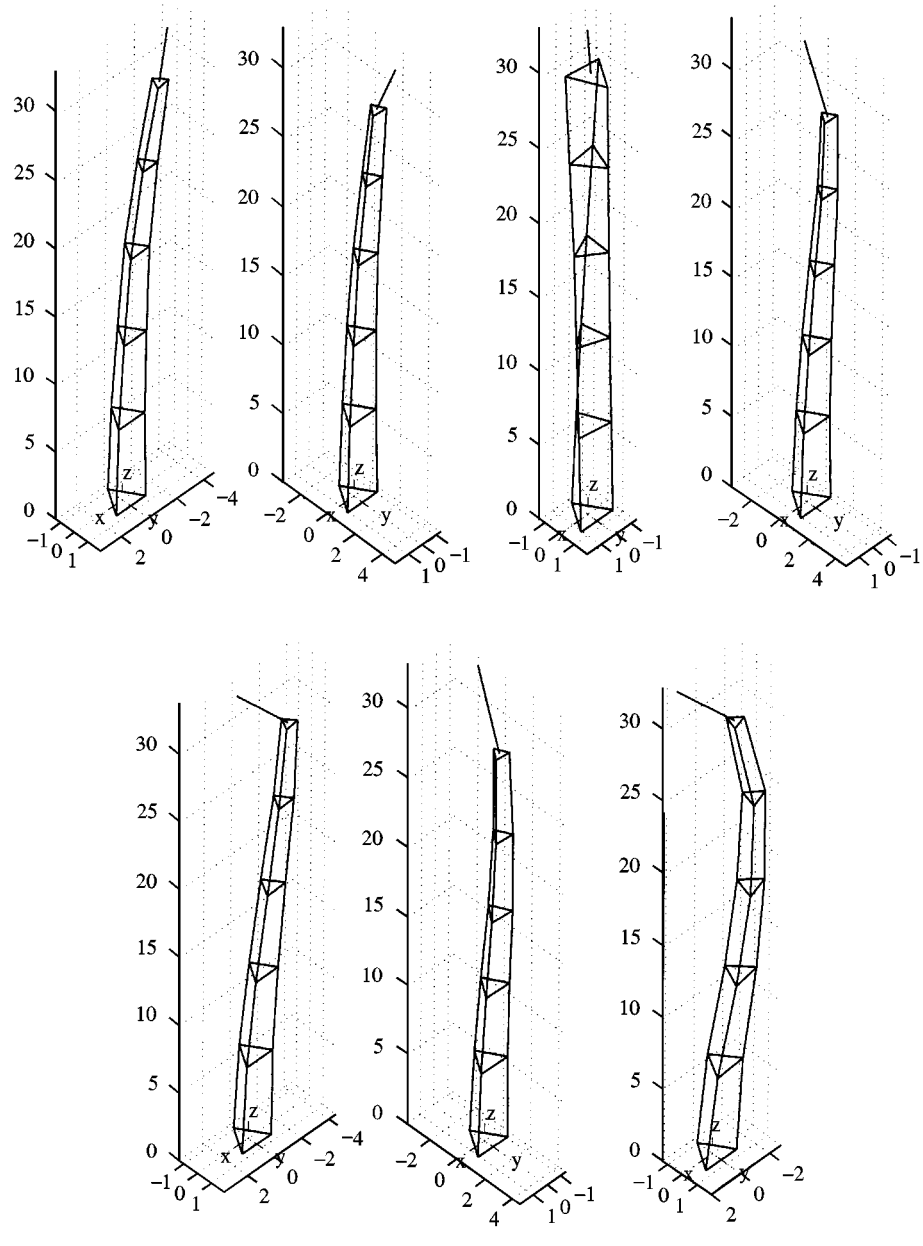

Figure 6. Mode shapes of the first 7 modes obtained with SSI/ref. In ascending order from left to right, from top to bottom.

40% of the computational time and number of floating point operations as required by SSI. The gain in computational efficiency is a function of the ratio r/l, the number of references over the total number of outputs. The mode shapes obtained with SSI/ref are represented in Fig. 6. If the MAC-matrix is computed between the SSI/ref and SSI mode shapes, diagonal values exceeding 99% are found for all seven modes, indicating that the identified modes are about the same for both methods.

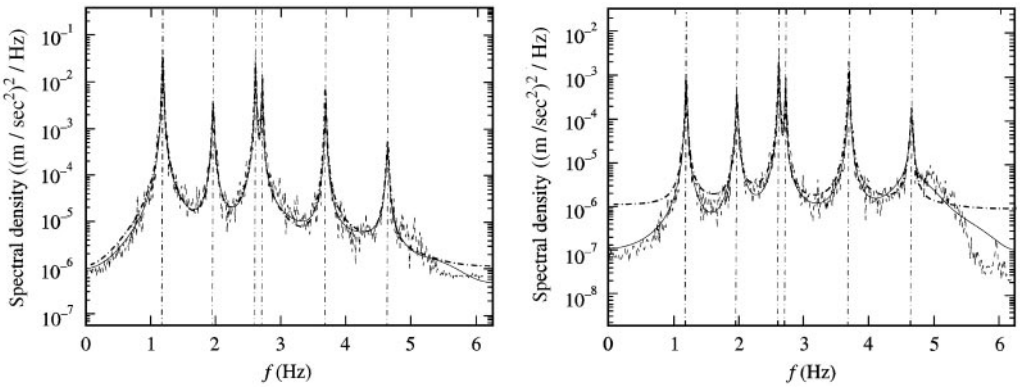

Figure. 7. Comparison of spectrum estimates. (left) Reference signal, (right) other signal. -, SSI, -.-., SSI/ref; - -, Welch's.

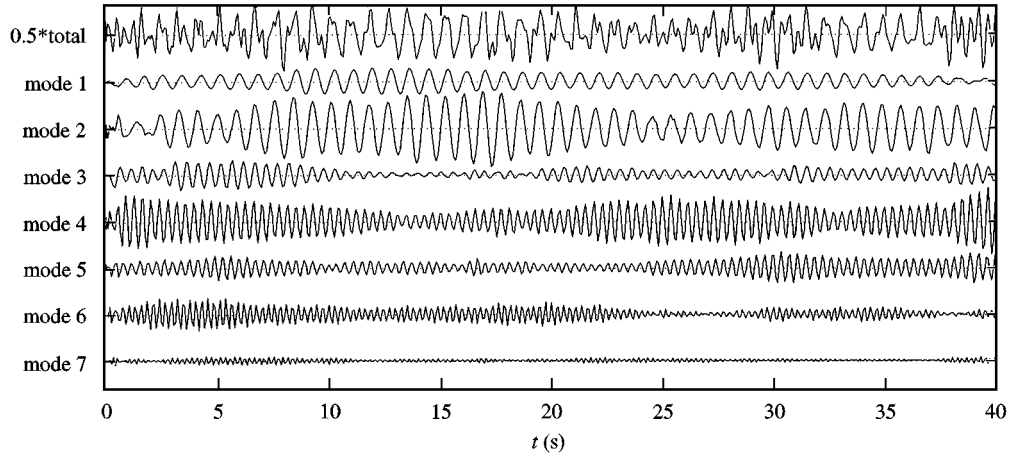

Figure 8. Modal contributions to the total response. The top chart is the measured data; the contributions from the first 7 modes are ordered from top to bottom. The amplitudes of the measured data have been multiplied by 0.5.

The stochastic state-space model can be converted analytically to an expression for the power and cross-spectra (53). These spectra can be compared with spectra that are obtained with a non-parametric identification method, e.g. Welch's averaged periodogram method that mainly consists of discrete Fourier transforms (DFT). In Fig. 7 the estimated power spectra of a reference channel and a non-reference channel are represented. Welch's spectrum is compared with the SSI/ref and the SSI spectrum. For the reference channel all spectra are well in line, but for the non-reference channel the SSI/ref spectrum differs from the other two. The resonance peaks are well described, but the valleys between the eigen-frequencies are different.

In Fig. 8 the approach of Section 6.3 has been used to determine the contributions of each mode to the total response. The differences between the top chart and the sum of the seven other charts are the residuals or one-step-ahead prediction errors (58). To obtain one number for each output channel, the total prediction error is defined as

$$\varepsilon_c = \sqrt{\frac{\sum_{k=1}^{N}((y_k)_c - (\hat{y}_k)_c)^2}{\sum_{k=1}^{N}((y_k)_c)^2}} \times 100\% \tag{59}$$

TABLE 2

Total prediction errors ε_c (%) for all nine output channels, obtained with two SSI/ref-cases: channels 1–3 as references and channels 2, 3, 8 as references and with SSI

Channel	1	2	3	4	5	6	7	8	9
SSI/ref (1–3)	**15**	**14**	**14**	17	17	24	23	23	25
SSI/ref (2, 3, 8)	17	**13**	**14**	18	13	24	22	**14**	27
SSI	13	13	14	13	13	18	13	14	14

where $(y_k)_c$ is channel c of the output vector. In Table 2, the prediction errors for SSI/ref with channels 1–3 as references, for SSI/ref with channels 2, 3, 8 as references and for classical SSI are presented. Note that channels 1–3 are the reference sensors common to every set-up and needed to obtain global mode shapes. There is however no theoretical objection against selecting different reference sensors in the identification of one set-up. In SSI/ref the prediction errors are lower for the reference channels and comparable with the classical SSI method. The prediction errors for the channels not belonging to the references are considerably higher.

9. CONCLUSIONS

This paper presented the use of stochastic subspace identification for in-operation modal analysis. A new implementation of the method was proposed: in the references based stochastic subspace identification method (SSI/ref), the row space of the future outputs is projected into the row space of the past reference outputs. This reduces the dimensions of the matrices and thus also the computation time. The new approach was illustrated and compared with the classical stochastic subspace identification method (SSI) using data from a vibration test on a steel transmitter mast. From this comparison the following conclusions can be made:

1. The SSI/ref method is considerably faster than SSI. Also the state-space model and related modal parameters are already stable at a lower model order. This increase in computational efficiency can be important in civil engineering applications where a structure is measured using a number of sensors and set-ups and where long data records are acquired.
2. Because of the difference set-ups, there are always overlapping reference sensors needed to obtain global mode shapes. The SSI/ref method incorporates the idea of the reference sensors already in the identification step.
3. The eigenfrequencies and damping ratios are determined with low and comparable uncertainties in both methods: SSI/ref and SSI. Also the mode shapes identified with both methods are about the same (MAC-values exceeding 99%).
4. The SSI/ref prediction errors are higher for channels that do not belong to the reference channels because these channels are partially omitted in the identification process. Also the spectrum derived from the SSI/ref state-space model deviates from Welch's DFT spectrum estimate for non-reference channels although the deviations are mainly situated between the resonance peaks and not at the resonances.
5. Some further investigations are still needed as to what extent the mode shapes suffer from the same fact, namely that the mode shape may be less accurately estimated at non-reference sensor positions. The MAC-values suggest that this is not the case, but it is

known that MAC is not able to indicate small changes. It will be investigated by the authors by means of a simulated example where the mode shapes are exactly known.

In addition to the determination of the modal parameters the subspace methods resulted in some interesting postprocessing/validation tools: an analytical expression for the spectra, the modal contributions to the total response and the prediction errors.

REFERENCES

1. C. KRÄMER, C. A. M. DE SMET and B. PEETERS 1999 *Proceedings of IMAC 17*, *Kissimmee*, *FL*, *USA*, 1030–1034. Comparison of ambient and forced vibration testing of civil engineering structures.
2. A. J. FELBER 1993 Ph.D. thesis, University of British Columbia, Vancouver, Canada. *Development of a hybrid bridge evaluation system.*
3. L. LJUNG 1987 *System Identification:Theory for the User*. Englewood Cliffs, NJ, USA: Prentice-Hall.
4. P. H. KIRKEGAARD and P. ANDERSEN 1997 *Proceedings of IMAC 15*, *Orlando*, *FL*, *USA*, 889–895. State space identification of civil engineering structures from output measurements.
5. B. PEETERS, G. DE ROECK and P. ANDERSEN 1999 *Proceedings of IMAC* 17, *Kissimmee*, *FL*, *USA*, pp. 231–237. Stochastic system identification: uncertainty of the estimated modal parameters.
6. P. VAN OVERSCHEE and B. DE MOOR 1991 *Proceedings of the 30th IEEE Conference on Decision and Control*, *Brighton*, *UK*, 1321–1326. Subspace algorithms for the stochastic identification problem.
7. A. BENVENISTE and J.-J. FUCHS 1985 *IEEE Transactions on Automatic Control* **AC-30**, 66–74. Single sample modal identification of a nonstationary stochastic process.
8. M. PREVOSTO, M. OLAGNON, A. BENVENISTE, M. BASSEVILLE and G. LE VEY 1991 *Journal of Sound and Vibration* **148**, 329–342. State space formulation: a solution to modal parameter estimation.
9. M. BASSEVILLE, A. BENVENISTE, B. GACH-DEVAUCHELLE, M. GOURSAT, D. BONNECASE, P. DOREY, M. PREVOSTO and M. OLAGNON 1993 *Mechanical Systems and Signal Processing* **7**, 401–423. In situ damage monitoring in vibration mechanics: diagnostics and predictive maintenance.
10. M. ABDELGHANI, M. BASSEVILLE and A. BENVENISTE 1997 *Proceedings of IMAC 15*, *Orlando FL*, *USA*, 1815–1821. In-operation damage monitoring and diagnostics of vibrating structures, with applications to offshore structures and rotating machinery.
11. L. MEVEL, M. BASSEVILLE, A. BENVENISTE, M. GOURSAT, M. ABDELGHANI and L. HERMANS 1999 *Proceedings of IMAC 17*, *Kissimmee*, *FL*, *USA*, *35–41.* On the application of a subspace-based fault detection method.
12. M. ABDELGHANI, M. GOURSAT, T. BIOLCHINI, L. HERMANS and H. VAN DER AUWERAER 1999 *Proceedings of IMAC 17*, *Kissimmee*, *FL*, *USA*, 224–230. Performance of output-only identification algorithms for modal analysis of aircraft structures.
13. L. HERMANS, H. VAN DER AUWERAER and L. MEVEL 1999 *Proceedings of IMAC 17*, *Kissimmee*, *FL*, *USA*, 42–48. Health monitoring and detection of a fatigue problem of a sports car.
14. C. HOEN, T. MOAN and S. REMSETH 1993 *Proceedings of EURODYN* '93, *the* 2*nd European Conference on Structural Dynamics*, *Trondheim*, *Norway*, 835–844. Rotterdam, Netherlands: A.A. Balkema. System identification of structures exposed to environmental loads.
15. P. GUILLAUME, L. HERMANS and H. VAN DER AUWERAER 1999 *Proceedings of IMAC 17*, *Kissimmee*, *FL*, *USA*, pp. 1887–1893. Maximum likelihood identification of modal parameters from operational data.
16. B. PEETERS, G. DE ROECK, L. HERMANS, T. WAUTERS, C. KRÄMER and C. A. M. DE SMET 1998 *Proceedings of ISMA 23*, *Leuven*, *Belgium*, 923–930. Comparison of system identification methods using operational data of a bridge test.
17. D. J. EWINS 1984 *Modal Testing*: *Theory and Practice*. Letchworth, Hertfordshire, UK: Research Studies Press.
18. J. N. JUANG 1994 *Applied system identification.* Englewood Cliffs, NJ, USA: Prentice Hall.
19. B. L. HO and R. E. KALMAN 1996 *Regelungstechnik* **14**, 545–548. Effective construction of linear state-variable models from input/output data.

20. H. AKAIKE 1974 *IEEE Transactions on Automatic Control* **19**, 667–674. Stochastic theory of minimal realization.
21. M. AOKI 1987 *State Space Modelling of Time Series*. Berlin, Germay: Springer-Verlag.
22. G.H. JAMES, T. G. CARNE and J. P. LAUFFER 1995 *Modal Analysis*: *the International Journal of Analytical and Experimental Modal Analysis* **10**, 260–277. The natural excitation technique (NExT) for modal parameter extraction from operating structures.
23. L. HERMANS and H. VAN DER AUWERAER 1998 *Proceedings of NATO/ASI. Sesimbra, Portugal.* Modal testing and analysis of structures under operational conditions: industrial applications.
24. P. VAN OVERSCHEE and B. DE MOOR 1996 *Subspace Identification for Linear Systems*: *Theory–Implementation–Applications*. Dordrecht, Netherlands: Kluwer Academic Publishers.
25. P. CAINES 1988 *Linear Stochastic Systems*. New York, USA: John Wiley & Sons.
26. T. BALENDRA 1993 *Vibration of Buildings to Wind and Earthquake Loads*. London, UK: Springer-Verlag.
27. B. PEETERS and G. DE ROECK 1998 *Proceedings of the IMAC 16, Santa Barbara, CA, USA*, 130–136. Stochastic subspace system identification of a steel transmitter mast.